The 248 nm Photodissociation of $ClNO_2$ Studied by Photofragment Translational Energy Spectroscopy

A. Furlan, M. A. Haeberli, and J. Robert Huber*

Physikalisch-Chemisches Institut der Universität Zürich,Winterthurerstrasse 190, CH-8057 Zürich, Switzerland

Received: March 1, 2000; In Final Form: June 21, 2000

The photodissociation of nitryl chloride ($ClNO_2$), a potentially active species in atmospheric chemistry, has been studied following excitation into the weakly structured band at 248 nm using photofragment translational energy spectroscopy. Among the energetically accessible decay channels, only the formation of the primary fragments Cl + NO_2 has been found to be active involving the fission of the weakest bond (D_0(Cl−NO_2) = 138 kJ/mol). The two fragments exhibit a well-structured translational energy distribution. The structure is attributed to different decay routes which include the formation of NO_2 fragments in different electronic states. Thus, about 30% are produced in the ground state while the rest, in accordance with the kinetic energy structure and the available fragment energy, is consistent with production in the A^2B_2 and B^2B_1 excited electronic states. The similar rovibrational energy channeled into NO_2 along the three decay routes suggests an indirect decay with an exit barrier. In addition, at high laser fluences secondary photodissociation of the hot or electronically excited NO_2 products to NO + O was observed.

1. Introduction

The destruction of the ozone layer has been attributed to the production of chlorine atoms in the stratosphere by photolysis of fluorochlorohydrocarbons.[1,2] In this context, other activated halogen compounds have been studied among which nitryl chloride, $ClNO_2$, has recently gained interest. This compound is formed in the marine boundary layer on sea salt aerosols involving the reaction $NaCl + N_2O_5 \rightarrow ClNO_2 + NaNO_3$[3] while in the rest of the troposphere it is the product of $HCl + N_2O_5 \rightarrow ClNO_2 + HNO_3$.[4] Although it is not known whether $ClNO_2$ is finally transported into the upper atmosphere or stratosphere, the elucidation of its photochemistry, which is expected to relate to that of the isovalent $HONO_2$, appears of interest.

Nitryl chloride is a planar molecule in its ground state (X^1A_1) with C_{2v} symmetry (see Figure 1a).[5] Its absorption spectrum, which is relatively weak above 200 nm, starts at around 380 nm. According to thermochemical data,[6] four dissociation processes might be active after absorption of a photon in the ultraviolet

$$ClNO_2 \rightarrow Cl + NO_2 \qquad \Delta H = 138 \text{ kJ/mol} \qquad (1)$$

$$\rightarrow ClO + NO \qquad \Delta H = 180 \text{ kJ/mol} \qquad (2)$$

$$\rightarrow ClNO + O \qquad \Delta H = 288 \text{ kJ/mol} \qquad (3)$$

$$\rightarrow Cl + O + NO \qquad \Delta H = 443 \text{ kJ/mol} \qquad (4)$$

The reaction enthalpies refer to the products in their electronic ground state.[6] It is, however, possible that they are created in electronically excited states which is not only relevant for the O and Cl atoms having low-lying spin−orbit excited states but also for the NO_2 molecule where the A^2B_2 and B^2B_1 states lie at 9726 and 14743 cm^{-1} above the X^2A_1 ground state, respectively.[7−9]

* Corresponding author. Tel: 0041-1-6354460. Fax: 0041-1-6356838. E-mail: jrhuber@pci.unizh.ch.

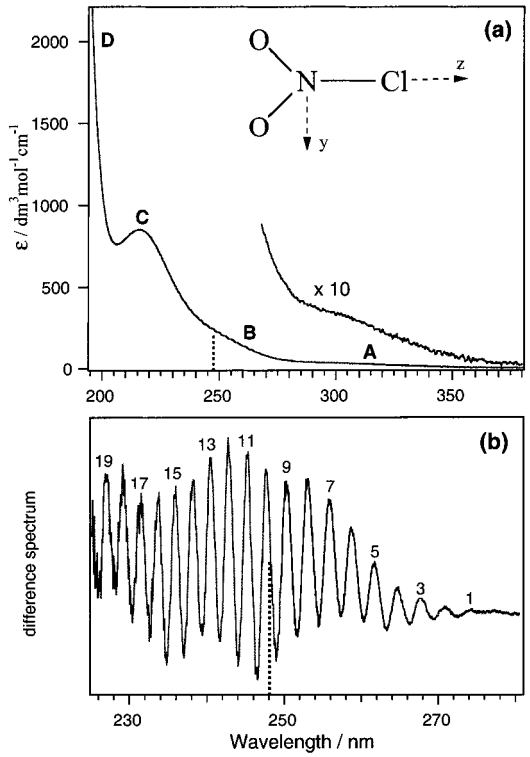

Figure 1. (a) Ultraviolet absorption spectrum of gas-phase nitryl chloride recorded at room temperature. The insert shows the structure of the molecule. (b) Enlarged view of the spectral region of interest. The unstructured background was subtracted after fit to a polynomial. The excitation wavelength is indicated by a dotted line.

Johnston and co-workers investigated the photolysis of $ClNO_2$ using a laser-induced fluorescence technique.[10] With excitation at 350 nm, rupture of the N−Cl bond was found to be the dominant decay process having a quantum yield of $\phi = 0.93 \pm 0.15$. Following dissociation at 308 and 235 nm, they observed fluorescence from the electronically excited NO_2 photoproduct;

10.1021/jp000792j CCC: $19.00
Published on Web 08/10/2000

the broad emission spectrum allowed no identification of the emitting state.[10] Using photofragment translational energy spectroscopy, Covinsky measured the kinetic energy distributions of the Cl, NO_2, NO, O, and ClNO fragments after irradiation at 248 nm.[11] In this unpublished work, he found three decay channels to be active, one leading to NO_2 in the ground state ($\phi = 0.32$) and one to an electronically excited state ($\phi = 0.66$) according to reaction 1. The third decay path to ClNO + O (3) was only of minor importance ($\phi = 0.02$). Very recently, Carter et al. studied the photodissociation of $ClNO_2$ by the REMPI-TOF method at 235 nm.[12] They observed a bimodal translational enery distribution for Cl from reaction 1 and assigned the two components to the decay channels leading to $NO_2(X^2A_1)$ with $\phi = 0.15 \pm 0.05$ and $NO_2(A^2B_2)$ with $\phi = 0.85 \pm 0.05$. The recoil anisotropy was measured to be $\beta = +1.1 \pm 0.1$, indicating that the excitation is predominantly to a state of A_1 symmetry (transition dipole along *z*) and the excited state lifetime is shorter than 2.2 ps.[12]

On the basis of these results we studied the photodissociation of $ClNO_2$ at 248 nm by photofragment translational energy spectroscopy (PTS). Applying low and high excitation laser fluences, primary and secondary photodissociation processes could be detected. Thus the different decay routes of reaction 1 leading to NO_2 in the ground and two electronically excited states were analyzed together with the secondary photochemical decay of the primary NO_2 product to NO + O.

2. Experiment

The time-of-flight (TOF) measurements were carried out with a photofragment translational energy spectrometer equipped with a rotatable molecular beam source described elsewhere.[13] Nitryl chloride, $ClNO_2$, was synthesized by passing HCl gas through a mixture of nitric and sulfuric acid and collecting the product in a low-temperature bath. Details of the synthesis, the purification, and storage of $ClNO_2$ are found in ref 14. At room temperature, and particularly in contact with metal, $ClNO_2$ undergoes slow decomposition which required the use of a metal-free inlet system and a Teflon-coated piezoelectric valve as described previously by Thelen et al.[15] From $ClNO_2$, stored at 77 K, a gas mixture of 17% $ClNO_2$ in He was prepared. This was expanded at a stagnation pressure of 350 mbar into the vaccuum chamber (10^{-7} mbar) and used within less than 4 h. During this time the small amount of developing contaminants ClNO, Cl_2, and NO_2, had a negligible effect on the measurement of the TOF spectra. Thus, following the experiment the concentration of the decomposition product ClNO in the inlet system was determined to be less than 3% using IR and UV spectroscopy and Cl_2 and NO_2 had no influence on the photodissociation owing to their low absorption cross section at 248 nm. The skimmed molecular beam pulses (cross section $\approx$7 mm^2) were crossed by the photolysis laser at a distance of 65 mm from the piezoelectric valve. Laser pulses at 248 nm were generated with a KrF excimer laser (Lambda Physik Compex 102) operated at 20 Hz. The laser beam was focused to an elliptical spot of about 6 mm^2 at the intersection with the molecular beam producing a laser fluence of about 2 J/cm^2. A part of the experiment was performed with a weaker focus resulting in a laser fluence of about 100 mJ/cm^2. The photodissociation products were detected at scattering angles $\Theta = 30°$, 45°, and 60°, where Θ is the angle between the molecular beam and the detection axis. After a flight path of 341 mm the fragments were ionized by electron bombardment and mass analyzed with a quadrupole mass filter (Balzers QMA 160). Depending on the count rate at a particular mass and scattering angle, the signal was averaged over $(1-3) \times 10^5$ laser shots to obtain a sufficiently high S/N ratio.

The molecular beam velocity distribution of $ClNO_2$ $f(v) \sim v^2 \exp[-(v - v_s)^2/\alpha^2]$ was determined before and after each measurement using a chopper wheel synchronized with the pulsed valve.[13] For the 17% mixture the stream velocity v_s and the width α were found to be 1110 and 72 m/s, respectively. A time offset of $3.9(m/e)^{1/2}$ μs has been subtracted in all of the TOF spectra in order to correct for the transit time of the ions through the mass filter.[13]

3. Results

A. Absorption Spectrum. The absorption spectrum of nitryl chloride at room temperature for the range 190−380 nm is shown in Figure 1a. The weak absorption between 300 and 400 nm is followed by an onset at $\approx$280 nm, a peak at 215 nm ($\epsilon_{215} \approx 850$ dm^3 mol^{-1} cm^{-1}) and a strong increase below 200 nm. Information in the literature about spectral assignments are sparse. Since ab initio calculation of the excited states of $ClNO_2$ are lacking, our tentative spectral assignments addressed in the Discussion section will rely on an analogy with related compounds such as $HONO_2$, results from photoelectron spectra of $ClNO_2$, and angular distributions of the recoiling photofragment Cl + NO_2. At the excitation wavelength of 248 nm used in this study the extinction coefficient is 236 dm^3 mol^{-1} cm^{-1} ($\sigma = 9 \times 10^{-19}$ cm^{-1}).

An enlarged view of the spectral region of interest for our study is displayed in Figure 1b. It represents the weak vibronic progression apparent in the range 220−280 nm and shows the modulated part of the absorption while the unstructured background was subtracted after fit to a polynomial. The progression has its origin at 274.2 nm (or 277.4 nm), an average spacing of 427 cm^{-1}, and peaks at around $v \approx 11$. The width of the bands is almost constant (fwhm = 215 ± 13 cm^{-1}) and much larger than our instrumental resolution of 15 cm^{-1}. Assuming purely homogeneous line broadening, this line width translates into an excited-state lifetime $\tau = h/(2\pi\Delta E_{fwhm}) \leq 25$ fs. Possible vibrational candidates of this excited-state progression are the O−N−O bending or the Cl−N stretching vibrations of $ClNO_2$ which both are of a_1 symmetry in C_{2v} (see below).

B. TOF Spectra. Photofragment spectra were recorded at the mass filter settings $m/e = 16$ (O^+), 30 (NO^+), 35 (Cl^+), 41 (ClO^+), 46 (NO_2), and 65 ($ClNO^+$). Signals were found at the ion masses of NO and Cl, but not at that of O^+, ClO^+, and $ClNO^+$. The signal at $m/e = 46$ (NO_2^+) was too weak to be analyzed. The small intensity of the NO_2^+ signal, compared to that of the Cl^+ counterfragment (reaction 1), can be attributed to extensive cracking of NO_2 in the ionizer. In a separate experiment we found that under the present experimental conditions NO_2 is detected as NO_2^+ and NO^+ in a ratio $NO_2^+/NO^+ \sim 0.2$ and for vibrationally or electronically excited NO_2 fragments even more extensive cracking to NO^+ is expected.

The TOF spectra monitored at $m/e = 35$ (Cl^+) with scattering angles $\Theta = 30°$, 45°, and 60° are shown in Figure 2. The solid lines represent the best fit obtained by forward convolution[16] of the center-of-mass kinetic energy distribution $P(E_T)$ of the fragments Cl + NO_2. The latter distribution is displayed in Figure 3. The TOF signals measured at $m/e = 30$ (NO^+) are shown in Figure 4. For a preliminary analysis we first assume that this signal is due to NO_2 produced as counterfragment to Cl and cracked in the ionizer to NO. Since the Cl and NO_2 product pairs are strictly momentum correlated, both fragments must have the same $P(E_T)$ after correction of the different masses. The thin solid line in Figure 4 was thus obtained from

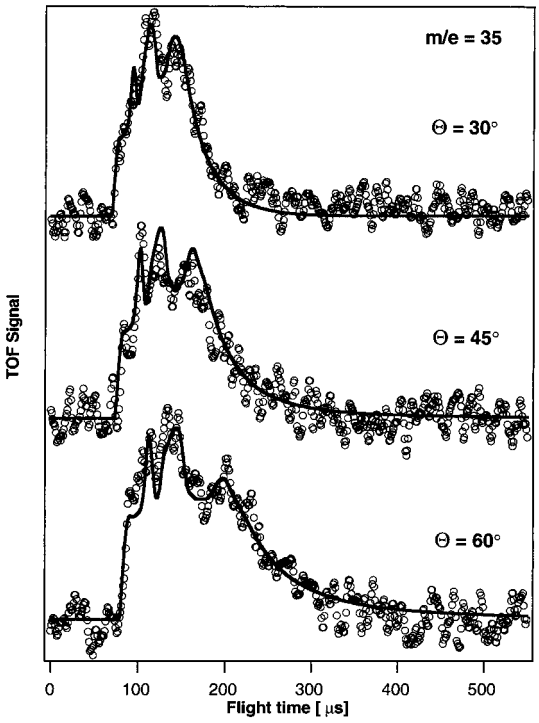

Figure 2. Photodissociation of $ClNO_2$ at 248 nm. Unpolarized TOF distributions measured at $m/e = 35$ (Cl^+) and scattering angles $\Theta = 30°$, 45°, and 60°. The solid line represents the best fit calculated with the $P(E_T)$ distribution shown in Figure 3.

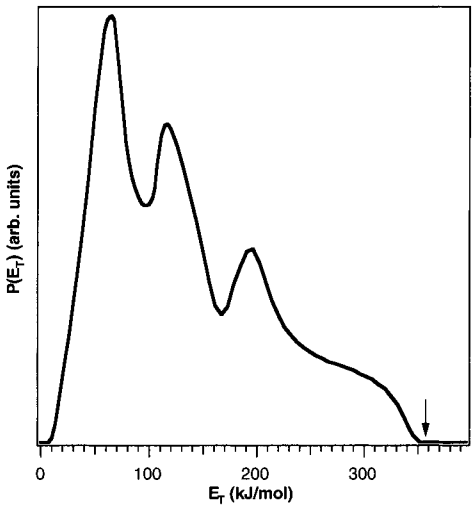

Figure 3. Center-of-mass translational energy distribution $P(E_T)$ of the fragments $Cl + NO_2$ from the photodissociation of $ClNO_2$ at 248 nm according to Figure 2. The arrow indicates the available energy of the fragment pairs.

the $P(E_T)$ shown in Figure 3. It is evident that this contribution from the decay to $Cl + NO_2$ reproduces only in part the observed NO^+ signal in Figure 4. The remaining signal may stem from three sources, namely a dissociation of $ClNO_2$ to $ClO + NO$ (2), a three-body decay to $Cl + O + NO$ (4), or a secondary decay of the primary photofragment NO_2 to $NO + O$ in a spontaneous or photoinduced mode. The decay to $ClO + NO$ can be excluded since ClO was not found as a photofragment. A three-body decay is possible in principle, but would yield very slow NO fragments due to the low available energy of $h\nu - D_0(Cl-NO_2) - D_0(O-NO) = 482 - 138 - 305$ kJ/mol = 39 kJ/mol. With a maximum kinetic energy of ≈10 kJ/mol these NO fragments are too slow to be detected under our experimental conditions and can therefore be neglected as contribution to the signal in Figure 4. A three-body decay induced by a *two-photon* absorption of $ClNO_2$ was also considered. The available energy released to the three fragments would in this case be sufficient to reproduce the fastest NO^+ signal in Figure 4. These fast fragments, however, should be formed in coincidence with fast Cl and O atoms. No O fragments were detected, and no Cl atoms were found to be faster than the limit given by the available energy after one-photon absorption of $ClNO_2$. Therefore, the three-body decay is concluded to be a negligible process under our experimental conditions. The spontaneous secondary decay of NO_2 fragments can only contribute to the NO^+ signal at long flight times and small scattering angles. The signal component due to spontaneous decay of NO_2 is displayed as dotted line in Figure 4 at $\Theta = 30°$, while at $\Theta = 45°$ and 60° this component is negligible. The details of the calculation for obtaining the secondary decay contribution have been descibed in detail elsewhere.[17,18] Briefly, the primary $P(E_T)$ is truncated at $E_T = 39$ kJ/mol which corresponds to the dissociation threshold for NO_2 in its ground electronic state. The NO_2 formed with a lower E_T constitute a fraction of ≈11% of all NO_2 fragments. This fraction has sufficient internal energy to decay to $NO + O$. For the secondary decay a $P(E_T)$ centered at 16 kJ/mol (fwhm = 8 kJ/mol) was chosen.

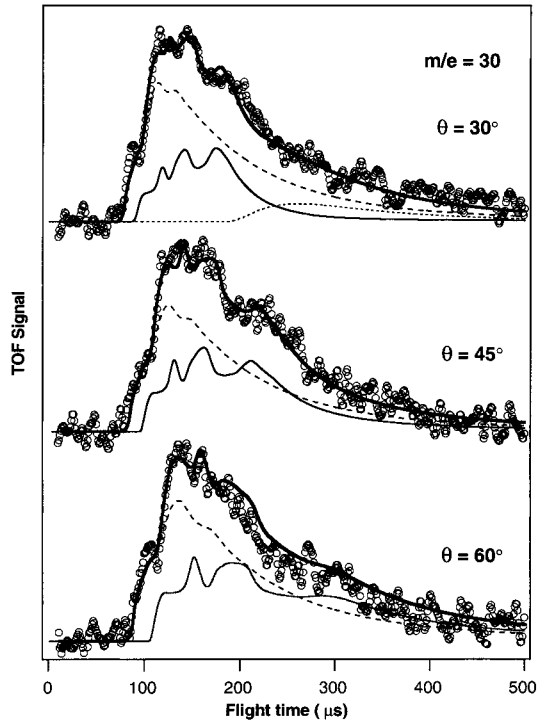

Figure 4. TOF distributions measured at $m/e = 30$ (NO^+) and scattering angles $\Theta = 30°$, 45°, and 60°. The thin solid lines represent the signal contribution from the primary decay of $ClNO_2$ to $Cl + NO_2$ according to the $P(E_T)$ distribution shown in Figure 3. The dashed lines denote the NO which stem from secondary photodissociation of nascent NO_2 fragments. NO from the spontaneous decay of nascent NO_2 only contributes to the spectrum recorded at $\Theta = 30°$ (dotted line). The bold solid lines represent the sum of all contributions.

Finally, we address the possibility of a *photoinduced* secondary dissociation of NO_2. Such a process requires a sufficiently high laser fluence and/or an appreciable absorption of NO_2. As noted above, the spectra shown in Figures 2 and 4 were recorded at a high laser fluence of ≈2 J cm^{-2}. The absorption cross section of NO_2 at *room temperature* and 248 nm is low (≈2 × 10^{-20} cm^2) but the primary NO_2 fragments are internally highly excited (see Discussion) which is expected to strongly increase

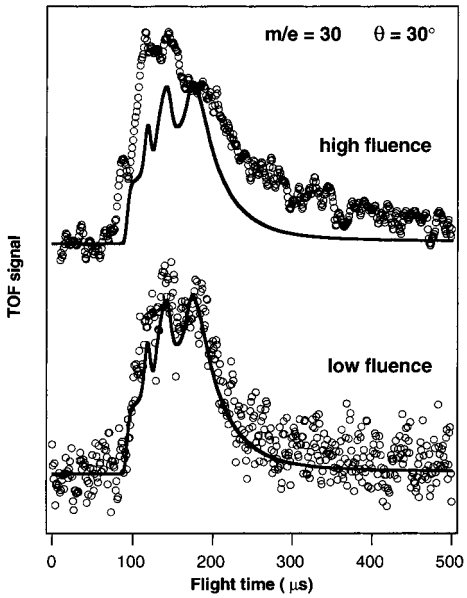

Figure 5. TOF distribution of NO^+ ($m/e = 30$, $\Theta = 30°$), recorded at a high and low laser fluence of 2 and 150 mJ cm^{-2}, respectively. The solid lines, obtained by forward convolution of the best fit with the primary $P(E_T)$ distribution (Figure 3), are in good agreement with the measured low fluence spectrum, while the high-fluence spectrum requires secondary decay of NO_2 to be taken into account.

the absorption cross section. Thus, we calculated the contribution of the secondary photodissociation to the NO^+ signal, indicated by dashed lines in Figure 4, by employing a roughly Gaussian-shaped secondary $P(E_T)$ distribution centered at around 90 kJ/mol with a half-width of ≈60 kJ/mol. To fit the scaling it was revealed that at our laser fluence 65% of the primary NO_2 fragments undergo secondary photodissociation. The sum of the signal of the primary NO^+ (thin solid line) and that of the secondary NO^+(dashed line) resulted in an excellent fit to the measured TOF spectrum (thick solid line). As the photoabsorption by NO_2 occurs after the decay of $ClNO_2$, the TOF spectra of Cl^+ are not affected by this secondary step.

If this analysis is correct, we expect at lower laser fluences two-photon processes to be reduced or even to disappear; i.e., the relative contribution to the NO^+ signal from secondary NO_2 dissociation should decrease with fluence. This was clearly observed, as demonstrated in Figure 5 which shows a high- and a low-fluence TOF measurement. The solid line in Figure 5, which represents exclusively the primary decay contribution (1) obtained with the $P(E_T)$ of Figure 3, is in good agreement with the low-fluence spectrum 5b, while in the high-fluence spectrum the secondary NO contribution is missing. In addition, we also confirmed that the laser fluence has no effect on the shape of the Cl^+ spectrum; the TOF measurements at low and high fluences yielded the same spectrum which is identical to those shown in Figure 2.

4. Discussion

A. Absorption Spectrum of $ClNO_2$. We start the discussion with an attempt to assign the two lowest electronic transitions denoted as band A and B in Figure 1. Excitation at 248 nm occurs into absorption B which shows a weak but distinct vibrational structure. Since results from calculations are not available, we base our assignment on a comparison with the isovalent nitric acid, $HONO_2$, a molecule whose photodissociation and absorption spectrum has been studied extensively in experiment[19−22] and theory.[23] Bai and Segal carried out ab initio calculations of the four lowest singlet states.[23] According to these calculations, the three lowest transitions of $HONO_2$ are all due to excitations from nonbonding orbitals on the NO_2 moiety to the NO_2 π^* lowest unoccupied orbital. Within the ONO_2 moiety this π^* orbital has a_2 symmetry in the C_{2v} group. The excitation of $HONO_2$ in the wavelength range 230−300 nm was assigned to an $n \rightarrow \pi^*$ transition to the first electronically excited singlet state of A_2 character.[19,23] Since this transition is electric dipole forbidden, vibronic mediation by an out-of-plane (a_2) vibration was proposed. This assignment is in agreement with the measured vector properties of the fragments OH + NO_2,[19] and in formal analogy to the well-known $n \rightarrow \pi^*$ transition in H_2CO.[24] Frost et al. measured the photoelectron spectra of various XNO_2 compounds (X = OH, F, Cl) and studied the effect of the X substituent in comparison with the spectral assignments and results from SCF calculations.[25] As in $HONO_2$, they confirmed that also in $ClNO_2$ the lowest unoccupied orbital has b_1 symmetry within C_{2v}. However, the highest occupied orbitals were found to be nonbonding chlorine orbitals (in-plane n_σ with b_2 symmetry, and out-of-plane n_π with b_1 symmetry), rather than n orbitals centered on the NO_2 moiety. As a consequence, the two lowest-energy transitions of $ClNO_2$ are expected to be from the A_1 ground state to an A_2 ($b_1 \otimes b_2$) and an A_1 ($b_1 \otimes b_1$) excited state, respectively. While the $A_1 \rightarrow A_2$ excitation is dipole forbidden, the $A_1 \rightarrow A_1$ transition is allowed with a transition dipole oriented parallel to the Cl−N bond axis. In their recent photodissociation measurements at 235 nm, Carter et al. found a preferential direction of the recoil velocities of the fragments Cl and NO_2 parallel to the polarization of the photolysis laser ($\beta = 1.1$),[12] a result similar to that obtained by Covinsky at 248 nm ($\beta \cong 0.95$)[11] using PTS. These recoil anisotropies are consistent only with a (preferentially) parallel $A_1 \rightarrow A_1$ transition, or a vibronically induced $A_1 \rightarrow A_2$ transition. Considering the appreciable absorption cross section of $\sigma(248\ \text{nm}) = 2 \times 10^{-17}$ cm^2 apparent in Figure 1, we tentatively assign the absorption B in the range 270−230 nm as being mainly due to the parallel $A_1 \rightarrow A_1$ transition, while the weaker absorption A at longer wavelengths is probably dominated by the vibronic $A_1 \rightarrow A_2$ transition. The vibrational structure in B is reminiscent of the Hartley band in ozone[26,27] or the lowest absorption band of CO_2[28] where a small structure is superimposed on a broad continuum. Following the interpretation of this spectral feature suggested for O_3 and CO_2, the initially prepared wave packet in the B state of $ClNO_2$ would be split into two parts, one that propagates directly into the exit channel along the N−Cl coordinate while the other one is temporarily trapped by the motion of a vibration probably associated with the NO_2 group. This motion is likely to be the totally symmetric NO_2 bending mode. In the electronic ground state it is found at 793 cm^{-1}, but excitation of an electron to a π^* orbital causes a weakening of the NO_2 bonds and in turn a reduction of the frequency to 427 cm^{-1}. (In the NO_2 molecule the corresponding frequency is 648 cm^{-1}.)[29] The long progression peaking at $v = 11$ would then imply a significant change in the O−N−O bond angle.

B. Energy Partitioning. Following the photoinduced cleavage of the $Cl-NO_2$ bond, the internal energy partitioned into the NO_2 fragment is given by

$$E_{int}(NO_2) = h\nu - D_0(Cl-NO_2) - E_T - E_{int}(ClNO_2) - E_{so}(Cl) \quad (5)$$

Here the excitation energy $h\nu$ is 482 kJ/mol, the dissociation

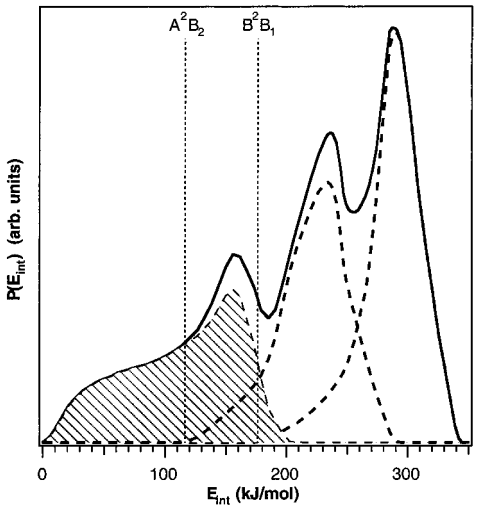

Figure 6. Internal energy distribution of the NO_2 fragments formed by photolysis of $ClNO_2$ derived by eq 5 from $P(E_T)$ in Figure 3. Guided by the structure, the $P(E_{int})$ distribution is partitioned into three components corresponding to NO_2 in the ground-state X^2A_1 (hatched area) and the first two excited states A^2B_2 and B^2B_1 (dashed lines). The band origins are indicated by vertical lines.

energy $D_0(Cl-NO_2) = 138$ kJ/mol,[6,12] and the spin−orbit splitting $E_{so}(Cl)$ is 10.5 kJ/mol (881 cm^{-1}). The internal energy of the parent molecule, $E_{int}(ClNO_2)$, can be set to zero in the cold environment of the supersonic jet. Applying eq 5 the kinetic energy distribution $P(E_T)$ in Figure 3 can be directly converted into the internal energy distribution of NO_2 fragments (=482 − 138 − E_T, kJ/mol) formed in coincidence with ground state $Cl(^2P_{3/2})$, as shown in Figure 6. (For spin−orbit excited chlorine, $Cl(^2P_{1/2})$, the $P(E_{int})$ distribution is then shifted by 10.5 kJ/mol to lower energies.)

Three distinct features with maxima around $E_{int} \approx 285$, 235, and 155 kJ/mol characterize the $P(E_{int})$ curve. It appears that three different types of NO_2 photofragments are created during dissociation which probably involve different electronic states of NO_2. In contrast to the present work, Carter et al.[12] found at 235 nm photolysis a bimodal distribution while the overall shape of the curve was similar to our result. This discrepancy can be attributed to the resolution. The PTS technique is in this respect superior to REMPI-TOF where resolving several narrow velocity components is challenging. In Figure 6 we present the result of an attempt to partition the total internal energy distribution into three components corresponding to NO_2 in the ground state X^2A_1 and the first two excited states A^2B_2 and B^2B_1. While the band origins (indicated by vertical lines in Figure 6) of the strongly vibronically perturbed A^2B_2 state (9726 cm^{-1})[7] and the linear B^2B_1 state (14 743 cm^{-1})[8] (and similar the D^2B_2 state at 16 849 cm^{-1})[8,9] are well-known, the positions of states which are optically inaccessible from the ground state, such as C^2A_2 ($\approx$16 200 cm^{-1})[30] and various quartet states,[31] are less well established.

Assuming such a partitioning of the NO_2 fragments into electronically excited species, the average rovibrational energy E_{rovib}, listed in Table 1, is found to be 121 kJ/mol in the ground electronic state, and 119 and 112 kJ/mol in the A and B excited states, respectively. As the available energy for a particularly created NO_2 electronic state increases in the order B → A → X, the rovibrational energy remains about constant and the translational energy increases. This situation is reminiscent of an indirect decay over an exit barrier, where the vibrational energy redistribution occurs mainly before the top of the barrier is reached and most of the potential energy beyond the barrier is impulsively released as product translation.[32] Thus, after absorption of a photon by NO_2Cl and redistribution of the internal energy on the dissociative potential energy surface, the translational motion of the departing Cl atom and the NO_2 group in the exit channel shows essentially no interaction with the vibational and rotational degrees of freedom. Along the three decay routes the electronic excitation of the NO_2 product occurs almost exclusively at the expense of the translational energy. (It is noted that the systematic energy partitioning in Table 1 is obtained only if we assume the formation of three NO_2 electronic states. An attempted analysis based on four electronic states (X, A, B, and C/D) clearly failed to provide such a consistent picture).

TABLE 1: Partitioning of Kinetic and Rovibrational Energy to Three Electronic States of NO_2: $E_{rovib} = h\nu - D_0 - E_T - E_{el}$[a]

assignment	E_{el}	E_{avl}	$\langle E_T \rangle$	$\langle E_{rovib} \rangle$	population (%)
NO_2 in X	0	344	223 (65%)	121 (35%)	≈28
NO_2 in A	116	228	108 (48%)	119 (52%)	≈33
NO_2 in B	176	168	56 (33%)	112 (67%)	≈39

[a] Energies are given in kJ/mol and in percent of the available energy, E_{avl}.

The fragment anisotropy measurement of Carter et al.[12] provided $\beta = 1.1 \pm 0.1$. Although only the β value of the slower NO_2 fragments (states A and B) could be measured with sufficient accuracy, the measurement of the fast component (state X) was found to be consistent with this value. The NO_2 products in the three different electronic states are therefore indicated to stem from the same dissociative state in agreement with the findings from the energy partitioning above. Furthermore, from the anisotropy factor a dissociation lifetime ≤2.2 ps was derived[12] which again is in agreement with the mechanistic picture proposed.

Finally, we compare the internal energy distribution of NO_2, Figure 6, with that of NO_2 fragments emerging from the photodissociation of related XNO_2 compounds. To this end the $P(E_{int})$ distributions of X + NO_2 fragments formed by photolysis of nitric acid ($HONO_2$),[21,22] chlorine nitrate ($ClONO_2$),[33] methyl nitrate (CH_3ONO_2),[34] and nitromethane (CH_3NO_2)[35] were analyzed. A remarkable difference is found between the distribution in Figure 6 and those of all other compounds XNO_2. While $P(E_{int})$ of Cl + NO_2 in Figure 6 extends down to zero internal energy, the lowest internal energies of all other fragment pairs X + NO_2 lie above ≈120 kJ/mol. Our results show that about 30% of the NO_2 fragments from $ClNO_2$ are formed in the electronic ground state. This fraction is given by the estimated area under the $P(E_{int})$ curves indicated by hatching. The lack of ground-state NO_2 formed from $HONO_2$, CH_3NO_2, and CH_3ONO_2, was attributed to an adiabatic correlation of the excited nπ* state of the parent molecule with $NO_2(A^2B_2)$ but not with the ground state $NO_2(X^2A_1)$.[22] However, for NO_2Cl where we expect at 248 nm a charge-transfer transition from Cl to the NO_2 unit,[25] the formation of $NO_2(X)$ is not restricted by such a correlation requirement.

5. Conclusions

The photodissociation of $ClNO_2$ was investigated at 248 nm. This wavelength lies in a region of the absorption spectrum which exhibits a weak, regular vibronic structure superimposed on a broad, unstructured background. The structure conforms to a long vibrational progression ($\langle \nu \rangle = 427$ cm^{-1}) which is tentatively assigned to the NO_2 bending mode in the excited state. Based on the electronic structure of $ClNO_2$,[25] the absorp-

tion at 248 nm is due to a partial charge-transfer excitation involving the promotion of a nonbonding electron of Cl into a π^* orbital on the NO_2 moiety.

From the decay channels (1−4), which are energetically accessible at the photon energy of 482 kJ/mol (248 nm), only the formation of the primary fragments Cl + NO_2 by scission of the weak Cl−NO_2 bond was found to be active. (The yield of reactions 2−4 was below the detection limit of our experiment of <3%.) The analysis of the TOF spectra of the Cl and NO fragments revealed a structured kinetic energy distribution consisting of three distinct peaks. All excess energy, obtained by subtracting the kinetic energy (and spin−orbit excitation of Cl) from the total available energy, is necessarily partitioned to the NO_2 fragment. Therefore, the structure of the internal energy distribution directly obtained from $P(E_T)$ is interpreted as reflecting the population of electronically excited states with their rovibrational excitations of the NO_2 fragments, which is in qualitative agreement with the previous emission work by Johnston et al.[10,11] and the REMPI-TOF study by Carter et al.[12] A fraction of about 30% of all NO_2 fragments is thereby formed in the electronic ground state X^2A_1, while the rest populates the excited electronic states A^2B_2 (≈30%) and B^2B_1 (≈40%).

At high laser fluences, secondary photodissociation of NO_2 was observed. Since the absorption cross section of cold ground state NO_2 at 248 nm is very low, the observed secondary decay confirms that most primary NO_2 fragments are internally hot or electronically excited, and hence exhibit a stronger absorption at this wavelength.

Acknowledgment. This work was supported by the Swiss National Science Foundation. The authors thank Rolf Pfister for the synthesis of nitryl chloride and Dr. Robert T. Carter for helpful discussions and critically reading the manuscript. J.R.H. is particularly grateful to Brad Moore for his continuous interest in our work and his generous hospitality during two sabbatical stays at UC Berkeley.

References and Notes

(1) Molina, M. J.; Rowland, F. S. *Nature* **1974**, *249*, 810.
(2) Behnke, W.; George, C.; Scheer, V.; Zetzsch, C. *J. Geophys. Res.* **1997**, *102*, 3795.
(3) Fickert, S.; Helleis, F.; Adams, J. W.; Moortgat, G. K.; Crowley, J. N. *J. Phys. Chem. A* **1998**, *102*, 10689.
(4) Finnlayson-Pitts, B. J.; Ezell, M. S., Jr.; J. N. P. *Nature* **1989**, *337*, 241.
(5) Endo, K. *Nippon Kagaku Kaishi* **1979**, *9*, 1129.
(6) *JANAF Thermochemical Tables*, Suppl. 1 ed., 1985; Vol. 14.
(7) Kirmse, B.; Delon, A.; Jost, R. *J. Chem. Phys.* **1998**, *108*, 6638.
(8) Hardwick, J. L.; Brand, J. C. D. *Chem. Phys. Lett.* **1973**, *21*, 458.
(9) Stevens, C. G.; Zare, R. N. *J. Mol. Spectrosc.* **1975**, *56*, 167.
(10) Nelson, H. H.; Johnston, H. S. *J. Phys. Chem.* **1981**, *85*, 3891.
(11) Covinsky, M. Thesis, University of California, Berkeley, 1991.
(12) Carter, R. T.; Hallou, A.; Huber, J. R. *Chem. Phys. Lett.* **1999**, *310*, 166.
(13) Felder, P. *Chem. Phys.* **1990**, *143*, 141.
(14) Volpe, M.; Johnston, H. S. *J. Am. Chem. Soc.* **1956**, *78*, 3903.
(15) Thelen, M.-A.; Felder, P.; Huber, J. R. *Chem. Phys. Lett.* **1993**, *213*, 275.
(16) Sparks, R. K.; Shobatake, K.; Carlson, L. R.; Lee, Y. T. *J. Chem. Phys.* **1981**, *75*, 3838.
(17) Zhao, X.; Nathanson, G. M.; Lee, Y. T. *Acta Physico-Chim. Sinica* **1992**, *8*, 70.
(18) Hintsa, E. J.; Zhao, X.; Lee, Y. T. *J. Chem. Phys.* **1990**, *92*, 2280.
(19) August, J.; Brouard, M.; Simons, J. P. *J. Chem. Soc., Faraday Trans. 2* **1988**, *84*, 587.
(20) Johnston, H. S.; Chang, S.-G.; Whitten, G. *J. Phys. Chem.* **1974**, *78*, 1.
(21) Felder, P.; Yang, X.; Huber, J. R. *Chem. Phys. Lett.* **1993**, *215*, 221.
(22) Myers, T. L.; Forde, N. R.; Hu, B.; Kitchen, D. C.; Butler, L. J. *J. Chem. Phys.* **1997**, *107*, 5361.
(23) Bai, Y. Y.; Segal, G. A. *J. Chem. Phys.* **1990**, *92*, 7479.
(24) Yamaguchi, Y.; Weselowski, S. S.; Huis, T. J. V.; III, H. F. S. *J. Chem. Phys.* **1998**, *108*, 5281.
(25) Frost, D. C.; Lee, S. T.; McDowell, C. A.; Westwood, N. P. C. *J. Electron Spectrosc. Relat. Phenom.* **1975**, *7*, 331.
(26) Johnson, B. R.; Kinsey, J. L. *J. Phys. Chem.* **1989**, *91*, 7638.
(27) Thelen, M.-A.; Gejo, T.; Harrison, J. A.; Huber, J. R. *J. Chem. Phys.* **1995**, *103*, 7946.
(28) Schinke, R.; Engel, V. *J. Chem. Phys.* **1990**, *93*, 3252.
(29) Herzberg, G. *Infrared and Raman spectra of polyatomic molecules*; Van Nostrand: New York, 1945.
(30) Aoki, K.; Hoshina, K.; Shibuya, K. *J. Chem. Phys.* **1996**, *105*, 2228.
(31) Gillispie, G. D.; Khan, A. U.; Wahl, A. C.; Hosteny, R. P.; Krauss, M. *J. Chem. Phys.* **1975**, *63*, 3425.
(32) North, S. W.; Blank, D. A.; Gezelter, J. D.; Longfellow, C. A.; Lee, Y. T. *J. Chem. Phys* **1995**, *102*, 4447.
(33) Nelson, C. M.; Moore, T. A.; Okumura, M.; Minton, T. K. *Chem. Phys.* **1996**, *207*, 287.
(34) Yang, X.; Felder, P.; Huber, J. R. *J. Phys. Chem.* **1993**, *97*, 10903.
(35) Lao, K. Q.; Jensen, E.; Kash, P. W.; Butler, L. J. *J. Chem. Phys.* **1990**, *93*, 3958.